BASIC SCIENCE

Streptozotocin-Induced Hyperglycemia Exacerbates Left Ventricular Remodeling and Failure After Experimental Myocardial Infarction

Tetsuya Shiomi, MD, Hiroyuki Tsutsui, MD, Masaki Ikeuchi, MD, Hidenori Matsusaka, MD, Shunji Hayashidani, MD, Nobuhiro Suematsu, MD, Jing Wen, MD, Toru Kubota, MD, Akira Takeshita, MD

Fukuoka, Japan

OBJECTIVES	The aim of the present study was to determine whether streptozotocin (STZ)-induced hyperglycemia exacerbates progressive left ventricular (LV) dilation and dysfunction after myocardial infarction (MI).
BACKGROUND	Diabetes mellitus (DM) adversely affects the outcomes in patients with MI. However, it is unknown whether DM can directly affect the development of post-MI LV remodeling and failure.
METHODS	Male mice were injected intraperitoneally with STZ (200 mg/kg; DM group) or vehicle only. At two weeks, MI was created in the STZ-injected (DM+MI group) or vehicle-injected mice (MI group) by left coronary artery ligation, and they were followed up for another four weeks.
RESULTS	Survival during six weeks was significantly lower in the DM+MI versus MI group (25% vs. 71%; p < 0.01), despite a similar infarct size (60 ± 2% vs. 61 ± 2%; p = NS). Echocardiography after two weeks of ligation showed LV dilation and dysfunction with MI, both of which were exaggerated in the DM+MI group. Likewise, LV end-diastolic pressure and lung weight were increased in mice with MI, and this increase was enhanced in the DM+MI group. The myocyte cross-sectional area in the non-infarcted LV increased to a similar degree in the DM+MI and MI groups, whereas the collagen volume fraction was greater in the DM+MI group. Deoxyribonucleic acid laddering was greater in the DM+MI group.
CONCLUSIONS	Hyperglycemia decreased survival and exaggerated LV remodeling and failure after MI by increasing interstitial fibrosis and myocyte apoptosis. Diabetes mellitus could be a risk factor for heart failure, independent of coronary artery lesions. (J Am Coll Cardiol 2003;42: 165–72) © 2003 by the American College of Cardiology Foundation

Diabetes mellitus (DM) is one of the greatest comorbid factors in patients with acute myocardial infarction (MI). Diabetic patients with MI have a higher incidence of death than do non-diabetic patients, both in the short-term phase and on long-term follow-up (1). The excess mortality of diabetic patients results primarily from the development of congestive heart failure (HF) and recurrent MI (2).

Myocardial infarction frequently produces progressive left ventricular (LV) dilation associated with hypertrophy of the non-infarcted LV. These changes in LV geometry, referred to as remodeling, contribute to the development of depressed cardiac function (3). Several mechanisms, whether alone or in combination, may adversely affect LV remodeling and failure after MI in patients with DM; such mechanisms include severe coronary artery disease (CAD), impaired vasodilatory reserve of coronary arteries, and pre-

existing LV dysfunction probably due to diabetic cardiomyopathy (4). Clinical studies in patients with acute MI have shown that the mortality is higher in diabetic patients, despite similar ejection fractions and similar coronary patency rates (5). These results raise the possibility that diabetes may adversely affect the LV remodeling process and lead to a higher incidence of HF among diabetic patients. However, it has been difficult to evaluate the impact of diabetes, per se, on post-MI remodeling in patients because of concomitant CAD. To overcome these limitations in clinical studies, we employed the animal model of HF due to MI by coronary artery ligation.

Therefore, the purpose of this study was to determine whether streptozotocin (STZ)-induced hyperglycemia exacerbates progressive LV chamber dilation and contractile dysfunction in a murine model of MI. Moreover, there is increasing evidence that myocyte hypertrophy and apoptosis in association with interstitial fibrosis are enhanced not only in diabetic (6) but also in post-MI hearts (7). Thus, we determined whether these remodeling processes may be mutually reinforcing in the setting of MI associated with diabetes, and DM may further enhance the development of HF.

Abbreviations and Acronyms	
ACE	= angiotensin-converting enzyme
CAD	= coronary artery disease
DM	= diabetes mellitus
DMTU	= dimethylthiourea
dP/dt	= rate of rise in left ventricular pressure
HF	= heart failure
LV	= left ventricle/ventricular
MCP	= monocyte chemoattractant protein
MI	= myocardial infarction
ROS	= reactive oxygen species
STZ	= streptozotocin
TGF	= transforming growth factor
TNF	= tumor necrosis factor

METHODS

Experimental design. The study was approved by our institutional Animal Research Committee and conformed to the Animal Care Guidelines of the American Physiological Society. Four groups of mice were studied in the present study. Diabetes mellitus was induced in male CD-1 mice (5 to 8 weeks old and 25 to 35 g body weight) by intraperitoneal injection of STZ (200 mg/kg body weight) (8,9). Tail vein blood glucose samples were measured five days after injection to ensure induction of diabetes. As a control, vehicle (0.1 mol/l citrate buffer, pH 4.5) was injected in another group of mice. At two weeks after injection, MI was created in STZ-injected (DM+MI group) or vehicle-injected mice (MI group) by ligating the left coronary artery (10). A sham operation without ligating the coronary artery was also performed in additional groups of STZ-injected (DM group) and saline-injected mice (control group). All four groups of mice (control, DM, MI, and DM+MI) were followed up for another two weeks (for two-week post-MI study) and four weeks (for six-week survival study).

EXPERIMENT 1: SIX-WEEK SURVIVAL STUDY. The survival analysis was performed in the control (n = 8), DM (n = 7), MI (n = 28), and DM+MI (n = 28) groups of mice. During the study period of six weeks (two weeks after vehicle or STZ injection and another four weeks after surgery), cages were inspected daily for deceased animals. All deceased mice were examined for the presence of pleural effusion and cardiac rupture.

EXPERIMENT 2: TWO-WEEK POST-MI STUDY. The following studies were performed in a separate experiment using groups of mice after four weeks (two weeks after vehicle or STZ injection and another two weeks after surgery).

Echocardiographic and hemodynamic measurements. Echocardiographic studies were performed under light anesthesia with tribromoethanol/amylene hydrate (Avertin; 2.5% wt/vol, 8 μl/g intraperitoneally) and spontaneous respiration. A two-dimensional parasternal short-axis view of the LV was obtained at the level of the papillary muscles.

In general, the best views were obtained with the transducer lightly applied to the mid to upper left anterior chest wall. The transducer was then gently moved cephalad or caudad and angulated until desirable images were obtained. After it was ensured that the imaging was on axis (based on the roundness of the LV cavity), two-dimensional targeted M-mode tracings were recorded at a paper speed of 50 mm/s. Under the same anesthesia with Avertin, a 1.4F micromanometer-tipped catheter (Millar Instruments, Houston, Texas) was inserted into the right carotid artery and then advanced into the LV to measure LV pressures (10). One subset of investigators (S.H. and N.S.), who were not informed of the experimental groups, performed in vivo LV function studies.

In our recent validation study (11), we reported excellent reliability of LV cavity dimension and fractional shortening measurements, in which an echocardiographic method similar to that used in this study was employed. The intraobserver and interobserver variabilities between two measurements divided by the mean value of the two measurements, expressed as a percentage, were <10%. The measurements made in the same animals on separate days were also highly reproducible. Therefore, our technique could be considered to allow noninvasive assessment of LV structure, even in mice with large MIs.

Tissue preparation and morphometric analysis. The heart was excised and dissected into the right and left ventricles, including the septum. The LV was cut into three transverse sections: apex, middle ring, and base. From the middle ring, 5-μm sections were cut and stained with Masson's trichrome. The boundary lengths of the infarcted and non-infarcted endocardial and epicardial surfaces were traced with a planimeter digital image analyzer. Infarct size (fraction of the infarcted LV) was calculated as the average of all slices and expressed as the percentage of circumference length (10). Myocyte cross-sectional area was determined by quantitative morphometry of tissue sections from the mid-LV (10). To measure collagen volume fraction, we stained collagens in paraffin-embedded tissue sections (5-μm thick) with sirius red (12). Briefly, the sections were rinsed with distilled water and treated with 0.1% picrosirius red solution in saturated, aqueous picric acid for 60 min. The sections were further washed in 0.01 mol/l HCl for 2 min, dehydrated, and mounted. Collagen fibers could be identified through polarization microscopy.

Apoptosis Assay. The myocardial tissues with MI were carefully dissected into three parts: the infarcted LV; the border-zone LV with the peri-infarct rim (1-mm rim of normal-appearing tissue); and the remaining non-infarcted (remote) LV. We examined whether apoptosis is present in the non-infarcted LV by the more sensitive ligation-mediated polymerase chain reaction (LM-PCR) fragmentation assays (ApoAlert LM-PCR ladder assay kit; Clonetech, Palo Alto, California) (13).

LV angiotensin-converting enzyme (ACE) activity, oxidative stress, and cytokine/chemokine gene expression. The following studies were performed using the non-infarcted LVs obtained from a separate group of additional control, DM, MI, and DM+MI mice treated identically, as described earlier.

Left ventricular ACE activity was measured by the rate of generation of His-Leu from a hippuryl-His-Leu substrate and expressed as nmol/mg tissue/h. The amount of reactive oxygen species (ROS) was quantified in LV tissues by electron spin resonance spectroscopy with 4-hydroxy-2,2,6,6-tetramethyl-piperidine-N-oxyl (hydroxy-TEMPO) (14). All measurements were performed in two parallel runs, in the presence and absence of the hydroxyradical scavenger, dimethylthiourea (DMTU). The expression level of genes, including transforming growth factor (TGF)-beta, tumor necrosis factor (TNF)-alpha, and monocyte chemoattractant protein (MCP)-1 was determined by a ribonuclease protection assay (15). The value of each hybridized probe was normalized to that of glyceraldehyde-3-phosphate-dehydrogenase in each template set as an internal control.

Plasma biochemical measurement. Before sacrifice, venous blood samples (1 ml) were collected for determination of plasma glucose, blood urea nitrogen (BUN), and aspartate aminotransferase (AST).

Statistical analysis. Data are expressed as mean ± SEM. Survival function estimates during the follow-up period were derived using the Kaplan-Meier method, and differences between groups were assessed by the log-rank test. Comparison of means between groups was performed by one-way analysis of variance, followed by post hoc *t* tests. The Bonferroni correction was done for multiple comparisons of means in the three groups of DM, MI, and DM+MI with that of the control group and between the MI and DM+MI groups. $p < 0.05$ was considered statistically significant.

RESULTS

Survival and blood chemistry. The mortality rates during 6 h after ligation were 3% and 7% in MI and DM+MI mice, respectively (p = NS). Survival rates during the study period were significantly lower in DM+MI versus MI mice (25% vs. 71%, $p < 0.01$) (Fig. 1). Death was suspected to be attributable to HF and/or arrhythmia. One DM+MI mouse (1%) and two MI mice (6%) died of LV rupture (p = NS).

Plasma glucose levels were elevated in both DM and DM+MI mice after STZ injection, compared with control mice (Table 1). Plasma BUN and AST, used to assess potential renal and hepatic toxicity, respectively, were not increased in the DM or DM+MI group (Table 1).

Infarct size. Infarct size, determined by histomorphometric analysis of LV sections at two weeks after MI, was comparable (60 ± 2% vs. 61 ± 2%; p = NS) between MI (n = 9) and DM+MI mice (n = 8). It was also comparable
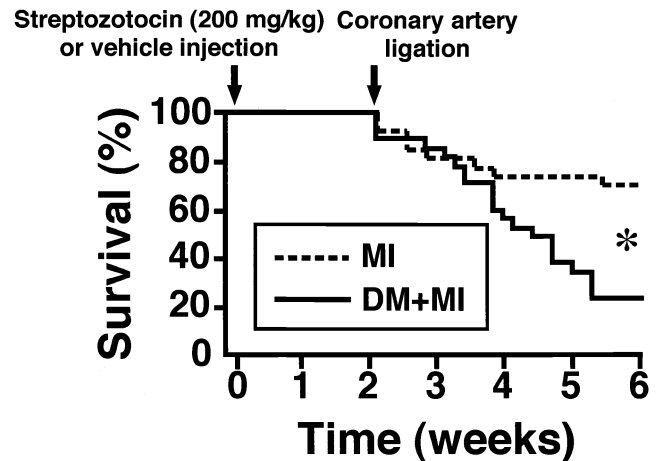

Figure 1. Kaplan-Meier survival analysis. Percentages of surviving diabetes mellitus (DM)+myocardial infarction (MI) (n = 28) and MI (n = 28) mice were plotted. Overall survival was significantly lower in DM+MI compared with MI mice. *p < 0.01 compared with the MI group.

(65 ± 2% vs. 59 ± 4%; p = NS) at three days after ligation, at which time the LV cavity size was similar between MI (n = 6) and DM+MI mice (n = 8).

Echocardiography and hemodynamics. Echocardiography at two weeks after surgery demonstrated that DM, per se, did not significantly affect LV diameter or shortening. In comparison with control mice, MI mice showed LV dilation and dysfunction, both of which were significantly exacerbated in the DM+MI group (Fig. 2 and Table 2).

Heart rate was comparable among all groups (Table 2). Mean aortic blood pressure was lower in the MI and DM+MI groups than in the control group, but there was no significant difference between these two groups. Left ventricular end-diastolic pressure was increased in the MI group and further enhanced in the DM+MI group. The maximum rate of rise in LV pressure (dP/dt_{max}) was decreased in the MI and DM+MI groups. Minimum dP/dt, an index of LV diastolic relaxation, was also lower in the MI group. This decrease tended to be exaggerated in the presence of DM, which, however, did not reach statistical significance (p = 0.09).

Organ weights. Body weight was lower in diabetic mice (Table 2), as previously observed (6,8). In contrast, the tibial length was similar among all groups. Coinciding with

Table 1. Blood Chemistry at Four Weeks After Streptozotocin or Vehicle Injection in Mice

	Control (n = 30)	**DM** (n = 33)	**MI** (n = 32)	**DM+MI** (n = 32)
Glucose (mg/dl)	117 ± 6	473 ± 16*	124 ± 8	416 ± 23*
BUN (mg/dl)	22.6 ± 1.5	27.9 ± 2.9	25.4 ± 1.2	29.6 ± 3.5
AST (IU/l)	35.2 ± 9.6	48.5 ± 8.4	34.4 ± 4.5	45.5 ± 8.3

*$p < 0.01$ vs. control. Data are means ± SEM.

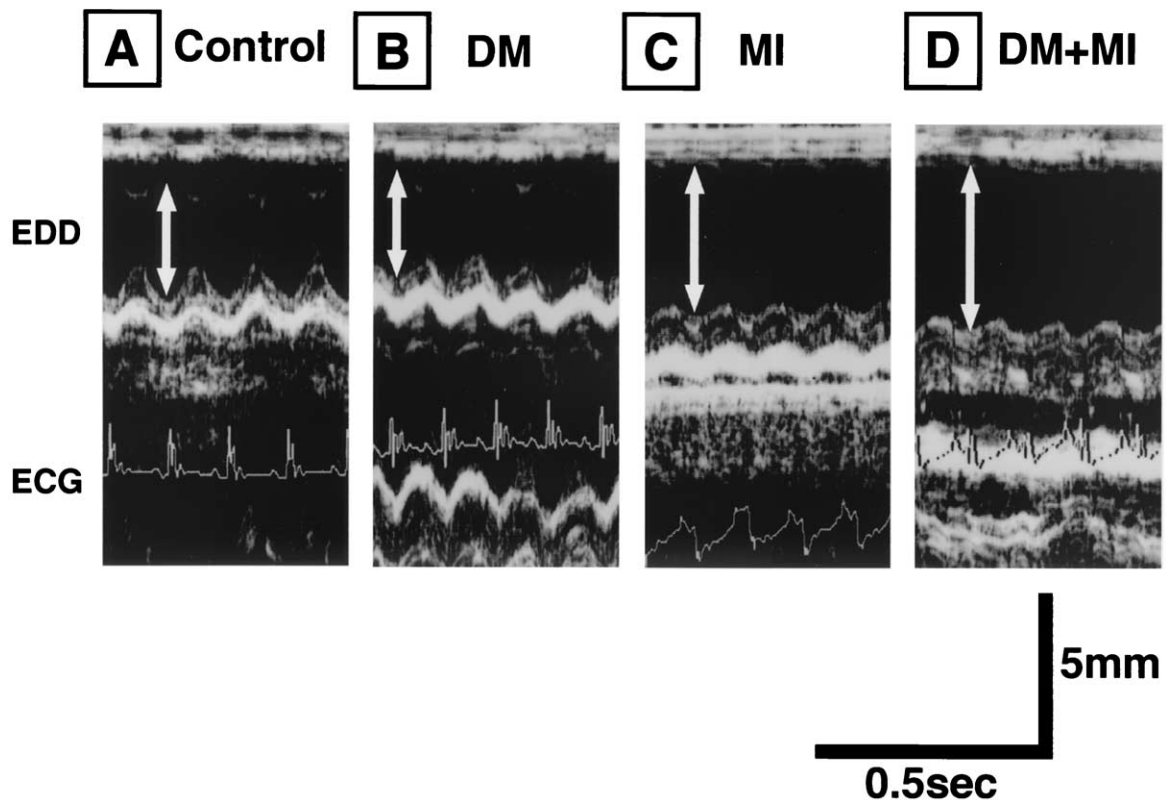AST = aspartate aminotransferase; BUN = blood urea nitrogen; DM = diabetes mellitus; MI = myocardial infarction.

Figure 2. M-mode echocardiograms obtained from a control **(A)**, diabetes mellitus (DM) **(B)**, myocardial infarction (MI) **(C)**, and DM+MI mouse **(D)** two weeks after surgery. EDD = end-diastolic diameter **(arrows)**. ECG = electrocardiogram.

increased LV end diastolic pressure, lung weight/tibial length was increased in the MI group, which was also exacerbated in the DM+MI group. The prevalence of pleural effusion was significantly higher in DM+MI than MI mice.

Histomorphometry. The myocyte cross-sectional area was significantly increased in DM, MI, and DM+MI mice compared with control mice (Figs. 3A and 3B). However, there was no significant difference in this parameter between MI and DM+MI mice. The collagen volume fraction was

Table 2. Echocardiographic, Hemodynamic Data, and Organ Weights of Mice

	Control	DM	MI	DM+MI
Echocardiographic data				
n	30	33	32	29
LVEDD (mm)	3.81 ± 0.03	3.72 ± 0.06	5.05 ± 0.05†	5.30 ± 0.06†§
LVESD (mm)	2.43 ± 0.04	2.40 ± 0.07	4.31 ± 0.05†	4.70 ± 0.07†§
Fractional shortening (%)	36.2 ± 0.6	35.5 ± 0.9	14.6 ± 0.4†	11.6 ± 0.4†§
Hemodynamic data				
n	29	29	27	27
Heart rate (beats/min)	460 ± 7	447 ± 6	452 ± 8	458 ± 12
Mean AoP (mm Hg)	79 ± 2	79 ± 2	68 ± 2†	69 ± 3*
LV EDP (mm Hg)	3.0 ± 0.5	4.8 ± 0.5	17.7 ± 1.3†	21.7 ± 1.5†‡
dP/dt$_{max}$ (mm Hg/s)	6,790 ± 228	6,519 ± 269	3,902 ± 208†	3,485 ± 221†
dP/dt$_{min}$ (mm Hg/s)	5,063 ± 150	4,425 ± 148†	2,962 ± 129†	2,485 ± 137†
Organ weights				
n	22	25	23	22
Body weight (g)	33.9 ± 0.7	29.0 ± 0.9†	30.9 ± 0.6*	26.0 ± 0.7†§
TL (mm)	21.1 ± 0.1	20.9 ± 0.1	21.1 ± 0.1	20.8 ± 0.1
LV weight/TL (mg/mm)	5.00 ± 0.12	3.91 ± 0.20†	4.86 ± 0.15	4.51 ± 0.15
RV weight/TL (mg/mm)	1.33 ± 0.04	1.14 ± 0.05	1.65 ± 0.09*	1.75 ± 0.10†
Lung weight/TL (mg/mm)	9.1 ± 0.1	8.2 ± 0.2	15.6 ± 1.0†	18.5 ± 1.2†‡
Pleural effusion (%)	0	0	28	53‡

*$p < 0.05$, †$p < 0.01$ vs. control. ‡$p < 0.05$, §$p < 0.01$ vs. MI. Data are means ± SEM.

AoP = aortic pressure; dP/dt = rate of rise in left ventricular pressure; EDD = end-diastolic diameter; EDP = end-diastolic pressure; ESD = end-systolic diameter; LV = left ventricular; RV = right ventricular; TL = tibial length; other abbreviations as in Table 1.
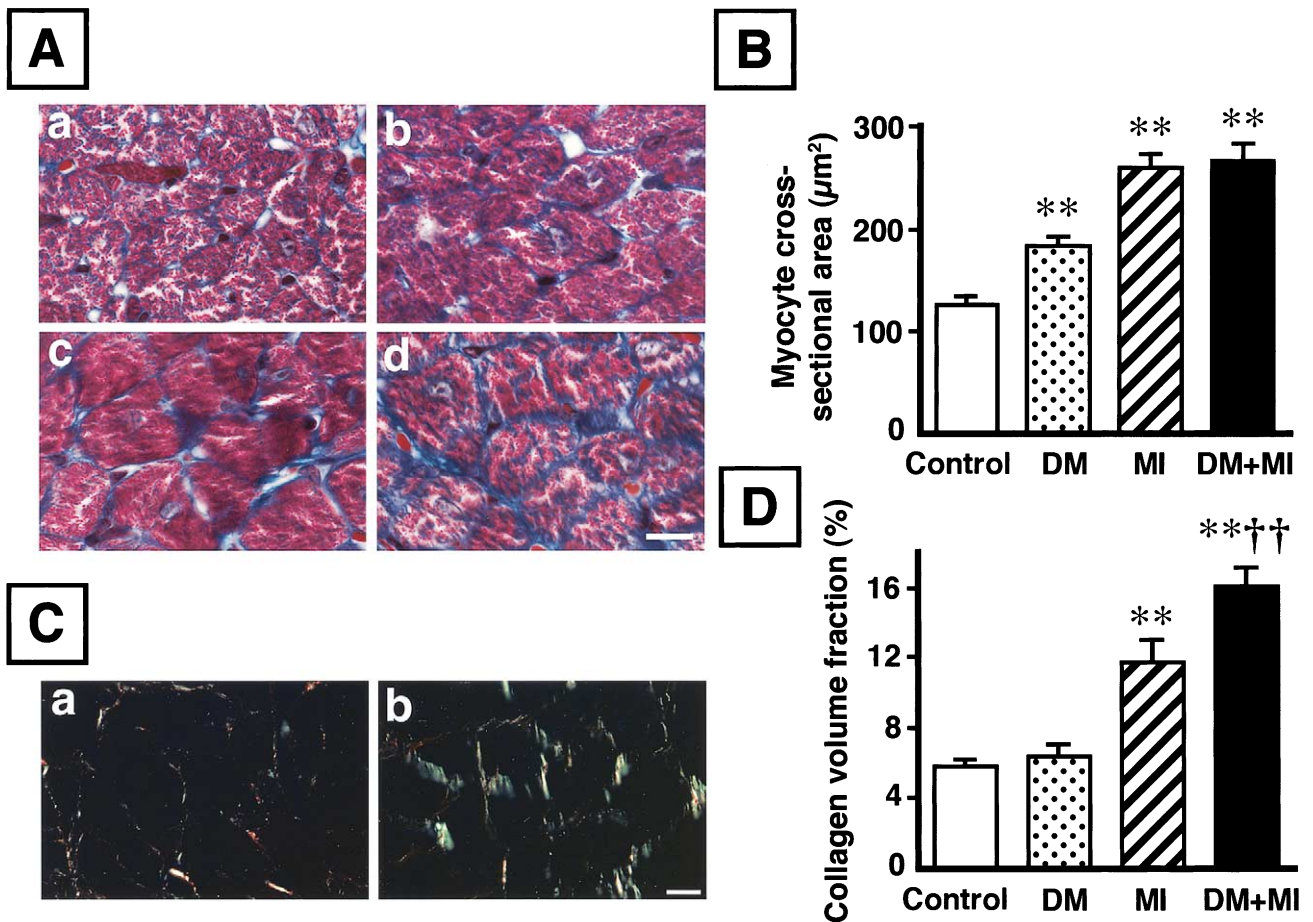
Figure 3. **(A)** Representative light microscopic photomicrographs of Masson's trichrome-stained myocardial sections obtained from control **(a)**, diabetes mellitus (DM) **(b)**, myocardial infarction (MI) **(c)**, and DM+MI **(d)** mice. Scale bar represents 10 μm. **(B)** Summarized data for myocyte cross-sectional area from control (n = 8), DM (n = 8), MI (n = 9), and DM+MI (n = 8) mice. **(C)** Representative light microscopic photomicrographs of sirius red-stained myocardial sections obtained from MI **(a)** and DM+MI **(b)** mice. Scale bar represents 10 μm. **(D)** Summarized data for collagen volume fraction from control (n = 6), DM (n = 6), MI (n = 6), and DM+MI (n = 6) mice. Values are means ± SEM. **p $<$ 0.01 compared with the control value; ††p $<$ 0.01 compared with the corresponding MI value.

also increased in MI and DM+MI mice, and this increase was significantly greater in DM+MI than MI mice (Figs. 3C and 3D).

Apoptosis. The intensity of the DNA ladder indicated that the apoptosis in the non-infarcted LV from DM+MI mice was further increased compared with that of MI mice (Fig. 4).

Cytokines, ACE, and ROS. Left ventricular ACE activity was significantly higher in the MI and DM+MI groups than in the control group (Table 3). However, it was comparable between the MI and DM+MI groups. The amount of ROS in the LV, expressed as the "DMTU-inhibitable" rate of electron spin resonance signal decay (14), was significantly greater in MI than control animals (Table 3). However, the extent of this increase was similar in DM+MI mice. Left ventricular gene expression of TGF-beta$_1$ was increased in MI mice and significantly exaggerated in DM+MI mice (Fig. 5). In addition, TNF-alpha and MCP-1 messenger ribonucleic acid levels were increased in MI mice and enhanced in DM+MI mice.
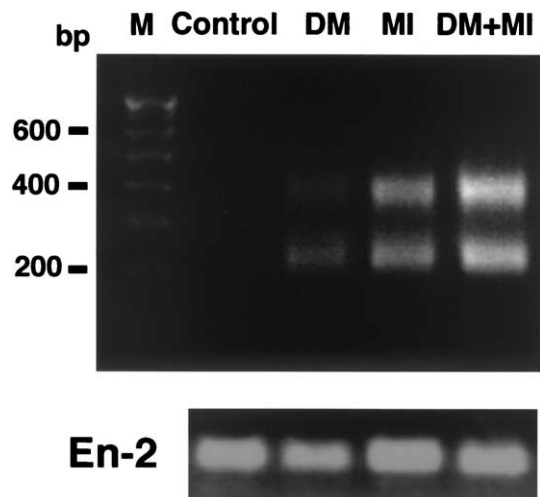

Figure 4. This deoxyribonucleic acid ladder indicative of apoptosis was detectable in the genomic deoxyribonucleic acid from the left ventricle. Apoptosis was further increased in the non-infarcted left ventricle of diabetes mellitus (DM)+myocardial infarction (MI) compared with MI mice. Amplification of the engrailed-2 (En-2) gene was performed as an internal control. bp = base pair; M = marker.

Table 3. Left Ventricular Angiotensin-Converting Enzyme Activity and Amount of Reactive Oxygen Species in Mice

	Control	DM	MI	DM+MI
ACE activity (nmol/mg per h)	21.5 ± 1.8 (n = 4)	12.7 ± 1.8 (n = 4)	56.0 ± 4.0* (n = 4)	51.6 ± 9.6* (n = 3)
ROS amount (/min)	0.012 ± 0.004 (n = 7)	0.017 ± 0.003 (n = 7)	0.021 ± 0.003† (n = 6)	0.021 ± 0.002† (n = 6)

*$p < 0.01$, †$p < 0.05$ vs. control. Data are means ± SEM.
    ACE = angiotensin-converting enzyme; ROS = reactive oxygen species; other abbreviations as in Table 1.

DISCUSSION

The major novel finding of this study was that MI mice had poor survival in the presence of DM. Diabetes mellitus decreased overall LV ejection performance, exacerbated LV remodeling, and increased chamber dilation as well as myocyte apoptosis and interstitial fibrosis of the non-infarcted myocardium. Therefore, this is the first report to provide evidence that hyperglycemia can exacerbate post-MI cardiac failure, even in the absence of CAD and hypertension.

Clinical relevance. In the present study, DM was associated with LV diastolic dysfunction characterized by decreased dP/dt_{min}. In contrast, normal systolic function was preserved in diabetic animals. Previous studies, despite some discrepancies, have demonstrated that, in general, DM presented with an early reduction in LV diastolic function, followed by progressive LV systolic failure (16,17). Furthermore, as previously demonstrated (18), DM alone increased myocyte size and interstitial fibrosis. However, the heart rate as well as LV size and systolic function were not altered in DM in the present study, which contrasts with some previous studies in rats (17,19). These differences might be due to differences in the species examined (mice vs. rats), the methods used to evaluate contractile function (in vivo vs. ex vivo), and the duration and severity of diabetes at which LV function was determined. Myocardial infarction produced LV cavity dilation associated with myocyte hypertrophy and interstitial fibrosis of non-infarcted LV. These changes, though significant, were modest compared with those seen in four-week post-MI animals (11).

A number of clinical studies have reported that the prognosis after MI is worse in diabetic patients who exhibit a higher incidence of HF and death than in non-diabetics (4). This may be due to the concomitant presence of severe coronary atherosclerotic lesions in diabetic patients. However, both experimental and clinical studies have shown that DM causes a specific form of myocardial damage independent of coronary atherosclerosis and manifests itself as LV dysfunction (20). In fact, STZ-induced diabetes has been shown to result in greater contractile dysfunction after ischemia and reperfusion (21). Therefore, a more likely explanation for the increased occurrence of HF in diabetic patients with MI is the exacerbation of LV remodeling due to DM. However, no previous studies have examined the impact of DM, per se, on post-MI remodeling and failure. Thus, the present study clearly demonstrates, using an animal model of MI caused by left coronary artery ligation, that hyperglycemia can exacerbate post-MI LV failure. Interestingly, despite a modest decline only in diastolic function from DM alone, diabetic mice developed severe systolic dysfunction after MI (Fig. 2 and Table 2).

Exacerbation of post-MI remodeling by DM. The deleterious effects of DM on myocardial function were not due to infarct expansion, because the infarct size was not altered at either three or 28 days after MI. It might be due to progressive LV dilation caused by remodeling of the remote region after healing of the infarct area. This LV remodeling process is caused by a number of mechanisms. The present results demonstrate that there was a significant increase in the collagen volume fraction—namely, interstitial fibrosis—in the non-infarcted LV of DM+MI compared with MI mice (Fig. 3). Another intriguing finding is the increase
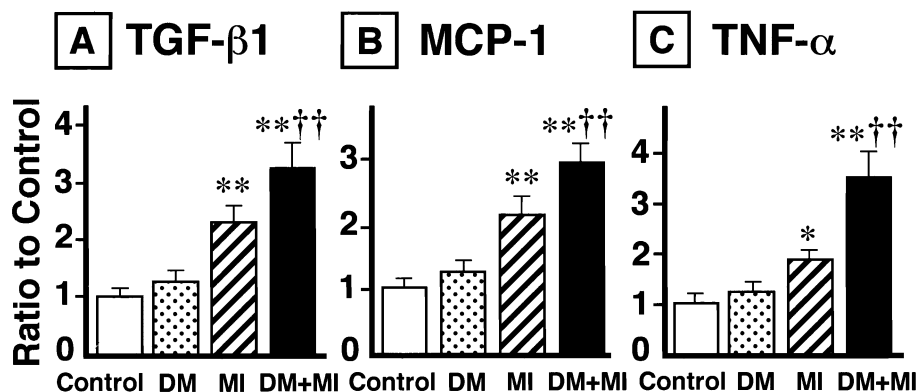

Figure 5. Densitometric analysis of transforming growth factor (TGF)-beta$_1$, tumor necrosis factor (TNF)-alpha, and monocyte chemoattractant protein (MCP)-1 gene expression in control (n = 8), diabetes mellitus (DM) (n = 9), myocardial infarction (MI) (n = 8), and DM+MI (n = 9) mice. Data were normalized by GAPDH concurrently run on the same gel and expressed as the ratio to control values. Values are means ± SEM. *$p < 0.05$, **$p < 0.01$ compared with the control value; ††$p < 0.01$ compared with the corresponding MI value.

of myocyte apoptosis in both the border and remote LV after MI (Fig. 4). This is consistent with previous studies showing the loss of myocytes as a result of apoptosis within the non-infarcted LV (22,23). Although the pathophysiologic significance of myocyte apoptosis in post-MI remodeling and failure remains mostly speculative (24), progressive loss of myocytes may lead to further deterioration of cardiac structure and function (25). Furthermore, the observed increase of interstitial fibrosis in DM+MI animals may also reflect an increase of cardiac myocyte death, which leads to more replacement fibrosis. Taken together, these observations suggest that exaggerated myocyte apoptosis and interstitial fibrosis may play an important role in the worsening of LV remodeling and failure in the presence of diabetes (26).

Next, we examined the stimulating factors responsible for enhanced interstitial fibrosis and apoptosis in the DM+MI mice. Recent studies have shown that the renin-angiotensin system is activated in diabetes (27). Therefore, diabetes and MI together may synergistically activate the renin-angiotensin system in the heart, which may further damage its function and structure. Another potential factor is oxidative stress, which has also been shown to be enhanced by hyperglycemia (28). Reactive oxygen species might be involved in the induction of TNF-alpha gene expression because hyperglycemia can produce ROS, which, in turn, have been shown to trigger TNF-alpha gene expression (29). However, there was no significant difference in the extent of increase in myocardial ROS measured by electron spin resonance techniques between MI and DM+MI mice (Table 3). Therefore, increased ROS production might not play a major role in the exacerbation of LV remodeling and failure in DM+MI mice. In addition, myocardial ACE activity was comparable between MI and DM+MI mice. The present study demonstrates that TGF-beta gene expression was increased in MI animals, which was significantly exaggerated in the DM+MI group (Fig. 5). Previous studies have shown that diabetes is associated with increased expression of TGF-beta (30). In addition, TGF-beta plays an important role in myocardial fibrosis. Therefore, one proposed mechanism by which DM exacerbates LV remodeling and failure is related to a further increase in TGF-beta after MI and the resultant enhancement of cardiac fibrosis. Interestingly, hyperglycemia significantly enhanced the gene expression of TNF-alpha and MCP-1 in post-MI hearts. The former (TNF-alpha) plays an important role in the pathogenesis of myocardial remodeling and failure (15). In addition, MCP-1 has been shown to be increased in failing hearts (31). Although the functional role of MCP-1 and its significance in myocardial failure remain unanswered, the upregulation of MCP-1 by DM could promote the further progression of HF. However, the present study does not provide direct proof of a cause-and-effect relationship between the increase of cytokine/chemokine expression and the exacerbation of LV failure by hyperglycemia. Further investigation is clearly needed.

Study limitations. There are several potential limitations to be acknowledged in this study. First, the amount of STZ used in the present study was based on previous reports in mice, in which 200 mg/kg body weight of STZ was used to induce hyperglycemia (8,9). These doses of STZ are higher than those used for rats (50 to 85 mg/kg) (17,19). This might probably be due to the different sensitivity to STZ between mice and rats. Plasma glucose levels in our animals were increased up to 400 to 500 mg/dl (Table 1). Although these values are similar to those reported by others in diabetic mice (500 to 600 mg/dl) (8,9) and in rats (500 mg/dl) (16–18), they are greater than those in rats after the injection of STZ 50 mg/kg body weight (267 mg/dl) (19). Therefore, the relatively higher plasma glucose levels in our animal model might contribute to the very poor outcome in the DM+MI mice and influence the clinical relevance of this study. Second, the decrease in insulin sensitivity is another important factor in DM and thus might play an important role in the exacerbation of post-MI remodeling and failure in the presence of DM. However, this crucial point was not examined in the present study.

Clinical implications. The present results may well explain the clinical observations that diabetes, per se, has a direct adverse impact on the outcomes of patients after MI (4). In addition to an acceleration of coronary atherosclerosis and an impairment of collateral formation, diabetes-induced exacerbation of LV remodeling and failure after MI is an important pathogenic mechanism responsible for this phenomenon. The findings in the present study may further draw attention to the early and intensive treatment of HF in diabetic patients with MI.

Conclusions. Streptozotocin-induced DM, independent of CAD, exacerbated LV remodeling and failure after MI. Myocyte apoptosis and interstitial fibrosis in post-MI hearts were increased in the presence of hyperglycemia, which might play an important role in the development of HF.

Reprint requests and correspondence: Dr. Hiroyuki Tsutsui, Department of Cardiovascular Medicine, Graduate School of Medical Sciences, Kyushu University, 3-1-1 Maidashi, Higashi-ku, Fukuoka, 812-8582 Japan. E-mail: prehiro@cardiol.med.kyushu-u.ac.jp.

REFERENCES

1. Haffner SM, Lehto S, Ronnemaa T, Pyorala K, Laakso M. Mortality from coronary heart disease in subjects with type 2 diabetes and in nondiabetic subjects with and without prior myocardial infarction. N Engl J Med 1998;339:229–34.
2. Woodfield SL, Lundergan CF, Reiner JS, et al. Angiographic findings and outcome in diabetic patients treated with thrombolytic therapy for acute myocardial infarction: the GUSTO-I experience. J Am Coll Cardiol 1996;28:1661–9.
3. Pfeffer MA, Braunwald E. Ventricular remodeling after myocardial infarction: experimental observations and clinical implications. Circulation 1990;81:1161–72.
4. Stone PH, Muller JE, Hartwell T, et al., the MILIS Study Group. The effect of diabetes mellitus on prognosis and serial left ventricular function after acute myocardial infarction: contribution of both coro-

nary disease and diastolic left ventricular dysfunction to the adverse prognosis. J Am Coll Cardiol 1989;14:49–57.

5. Granger CB, Califf RM, Young S, et al., the Thrombolysis and Angioplasty in Myocardial Infarction (TAMI) Study Group. Outcome of patients with diabetes mellitus and acute myocardial infarction treated with thrombolytic agents. J Am Coll Cardiol 1993;21:920–5.

6. Dhalla NS, Liu X, Panagia V, Takeda N. Subcellular remodeling and heart dysfunction in chronic diabetes. Cardiovasc Res 1998;40:239–47.

7. Cleutjens JP, Verluyten MJ, Smiths JF, Daemen MJ. Collagen remodeling after myocardial infarction in the rat heart. Am J Pathol 1995;147:325–38.

8. Kanki H, Fukuda K, Okushi K, et al. Comparison of nerve growth factor mRNA expression in cardiac and skeletal muscle in streptozotocin-induced diabetic mice. Life Sci 1999;65:2305–13.

9. Katoh M, Ohmachi Y, Kurosawa Y, Yoneda H, Tanaka N, Narita H. Effects of imidapril and captopril on streptozotocin-induced diabetic nephropathy in mice. Eur J Pharmacol 2000;398:381–7.

10. Hayashidani S, Tsutsui H, Shiomi T, et al. Fluvastatin, a 3-hydroxy-3-methylglutaryl coenzyme A reductase inhibitor, attenuates left ventricular remodeling and failure after experimental myocardial infarction. Circulation 2002;105:868–73.

11. Shiomi T, Tsutsui H, Hayashidani S, et al. Pioglitazone, a peroxisome proliferator-activated receptor-gamma agonist, attenuates left ventricular remodeling and failure after experimental myocardial infarction. Circulation 2002;106:3126–32.

12. Namba T, Tsutsui H, Tagawa H, et al. Regulation of fibrillar collagen gene expression and protein accumulation in volume-overloaded cardiac hypertrophy. Circulation 1997;95:2448–54.

13. Kubota T, Miyagishima M, Frye CS, et al. Overexpression of tumor necrosis factor-alpha activates both anti- and pro-apoptotic pathways in the myocardium. J Mol Cell Cardiol 2001;33:1331–44.

14. Ide T, Tsutsui H, Kinugawa S, et al. Direct evidence for increased hydroxyl radicals originating from superoxide in the failing myocardium. Circ Res 2000;86:152–7.

15. Kubota T, Bounoutas GS, Miyagishima M, et al. Soluble tumor necrosis factor receptor abrogates myocardial inflammation but not hypertrophy in cytokine-induced cardiomyopathy. Circulation 2000; 101:2518–25.

16. Mihm MJ, Seifert JL, Coyle CM, Bauer JA. Diabetes related cardiomyopathy time dependent echocardiographic evaluation in an experimental rat model. Life Sci 2001;69:527–42.

17. Hoit BD, Castro C, Bultron G, Knight S, Matlib MA. Noninvasive evaluation of cardiac dysfunction by echocardiography in streptozotocin-induced diabetic rats. J Card Fail 1999;5:324–33.

18. Grimm D, Jabusch HC, Kossmehl P, et al. Experimental diabetes and left ventricular hypertrophy: effects of beta-receptor blockade. Cardiovasc Pathol 2002;11:229–37.

19. Joffe II, Travers KE, Perreault-Micale CL, et al. Abnormal cardiac function in the streptozotocin-induced non-insulin-dependent diabetic rat: noninvasive assessment with Doppler echocardiography and contribution of the nitric oxide pathway. J Am Coll Cardiol 1999;34: 2111–9.

20. Malhotra A, Reich D, Nakouzi A, Sanghi V, Geenen DL, Buttrick PM. Experimental diabetes is associated with functional activation of protein kinase C epsilon and phosphorylation of troponin I in the heart, which are prevented by angiotensin II receptor blockade. Circ Res 1997;81:1027–33.

21. Paulson DJ. The diabetic heart is more sensitive to ischemic injury. Cardiovasc Res 1997;34:104–12.

22. Bialik S, Geenen DL, Sasson IE, et al. Myocyte apoptosis during acute myocardial infarction in the mouse localizes to hypoxic regions but occurs independently of p53. J Clin Invest 1997;100:1363–72.

23. Sam F, Sawyer DB, Chang DL, et al. Progressive left ventricular remodeling and apoptosis late after myocardial infarction in mouse heart. Am J Physiol Heart Circ Physiol 2000;279:H422–8.

24. Schaper J, Elsasser A, Kostin S. The role of cell death in heart failure. Circ Res 1999;85:867–9.

25. Anversa P, Leri A, Beltrami CA, Guerra S, Kajstura J. Myocyte death and growth in the failing heart. Lab Invest 1998;78:767–86.

26. Weber KT. Extracellular matrix remodeling in heart failure: a role for de novo angiotensin II generation. Circulation 1997;96:4065–82.

27. Fiordaliso F, Li B, Latini R, et al. Myocyte death in streptozotocin-induced diabetes in rats is angiotensin II-dependent. Lab Invest 2000;80:513–27.

28. Tanaka Y, Gleason CE, Tran PO, Harmon JS, Robertson RP. Prevention of glucose toxicity in HIT-T15 cells and Zucker diabetic fatty rats by antioxidants. Proc Natl Acad Sci USA 1999;96:10857–62.

29. Aikawa R, Nitta-Komatsubara Y, Kudoh S, et al. Reactive oxygen species induce cardiomyocyte apoptosis partly through TNF-alpha. Cytokine 2002;18:179–83.

30. Rumble JR, Cooper ME, Soulis T, et al. Vascular hypertrophy in experimental diabetes: role of advanced glycation end products. J Clin Invest 1997;99:1016–27.

31. Shioi T, Matsumori A, Kihara Y, et al. Increased expression of interleukin-1-beta and monocyte chemotactic and activating factor/monocyte chemoattractant protein-1 in the hypertrophied and failing heart with pressure overload. Circ Res 1997;81:664–71.